Impact of energy straggle on proton-induced single event upset test in a 65-nm SRAM cell*

Bing Ye(叶兵)[1,2,3], Jie Liu(刘杰)[1,†], Tie-Shan Wang(王铁山)[3], Tian-Qi Liu(刘天奇)[1,2], Jie Luo(罗捷)[1,2], Bin Wang(王斌)[1,2], Ya-Nan Yin(殷亚楠)[1,2], Qing-Gang Ji(姬庆刚)[1,2], Pei-Pei Hu(胡培培)[1,2], You-Mei Sun(孙友梅)[1], and Ming-Dong Hou(侯明东)[1]

[1] *Institute of Modern Physics, Chinese Academy of Sciences, Lanzhou* 730000, *China*
[2] *University of Chinese Academy of Sciences (UCAS), Beijing* 100049, *China*
[3] *Lanzhou University, Lanzhou* 730000, *China*

(Received 13 March 2017; revised manuscript received 25 April 2016; published online 20 June 2017)

This paper presents a simulation study of the impact of energy straggle on a proton-induced single event upset (SEU) test in a commercial 65-nm static random access memory cell. The simulation results indicate that the SEU cross sections for low energy protons are significantly underestimated due to the use of degraders in the SEU test. In contrast, using degraders in a high energy proton test may cause the overestimation of the SEU cross sections. The results are confirmed by the experimental data and the impact of energy straggle on the SEU cross section needs to be taken into account when conducting a proton-induced SEU test in a nanodevice using degraders.

Keywords: single event upset, energy straggle, proton irradiation, nanodevice

PACS: 85.30.De, 61.82.Fk, 25.40.Ep **DOI:** 10.1088/1674-1056/26/8/088501

1. Introduction

When a proton-induced single event upset (SEU) experiment is carried out, it is very important how the required proton energies are gained. There are usually two options: one is adjusting the parameters of the accelerator, and the other method is changing the thickness of the degraders. The first method can gain a more monochromatic proton beam, however it will take a certain amount of time to adjust the accelerator (generally it takes at least an hour, compared with a few minutes to change the degrader) and reduce the experiment efficiency greatly. Besides, some required proton energies are not available by adjusting the accelerator due to the design limitations of the facility. Therefore, a degrader has been extensively used to obtain the required proton energies on the basis of a certain initial energy of proton beam. The most commonly used degraders are aluminum (Al) and copper (Cu).

In 2008, Heidel *et al.* used 148-MeV primary proton beam energy at the Francis H. Burr Northeast Proton Therapy Center and obtained a wide proton energy range from 30 MeV to 148 MeV through adding degraders.[1] In 2011, Loveless *et al.* also used only one primary proton beam energy to gain various proton energies from 1 MeV to 100 MeV through a degrader block positioned at a variable distance away from the beam port.[2] There are also many other examples that use the degrader to obtain different proton energies from the primary proton beam.[3–10] However, the use of degraders will cause the range and energy to straggle and then have an influence on the result of the SEU test, but not enough attention has been paid to the impact of the degrader on proton-induced SEU experiments. Therefore, this paper examined the applicability of a degrader and the impact of energy straggle on a proton-induced SEU test. In this paper, SRIM-2008[11] simulated results on proton range straggle for different degraders were presented. In addition, the geometrical model has been established based on the real nano-SRAM device. The impact of energy straggle on the deposited charge in sensitive volume (SV) and SEU cross section was investigated by CRÈME-MC[12] simulation.

2. Simulation of SRAM cell

In this paper, the CRÈME-MC Monte Carlo simulation method was used to calculate the deposited charge in SV. Figure 1(a) shows the cross-section scanning electron microscopy (SEM) diagram of the static random access memory (SRAM) device fabricated in CYPRESS 65-nm process. A multi-layer cubic model (10 μm × 10 μm × 10 μm) was constructed in CRÈME-MC according to the SEM picture and elemental analysis of the chip. The 8-layer structure contained 3 SiO_2 layers, 3 copper layers, and 1 tungsten layer, as shown in Fig. 1(b).

Heavy ion experiment result[13] shows that the threshold linear energy transfer (LET) of an SRAM cell fabricated in CYPRESS 65-nm process is 0.13 MeV·cm^2/mg. So, we chose the critical charge (Q_c) of the device as 1.35 fC according to the following formula

$$Q_c(\mathrm{fC}) = 10.35 \times \mathrm{LET_{th}} \times D_{\mathrm{SV}}(\mu\mathrm{m}). \quad (1)$$

*Project supported by the National Natural Science Foundation of China (Grant Nos. 11690041 and 11675233).
†Corresponding author. E-mail: j.liu@impcas.ac.cn
© 2017 Chinese Physical Society and IOP Publishing Ltd

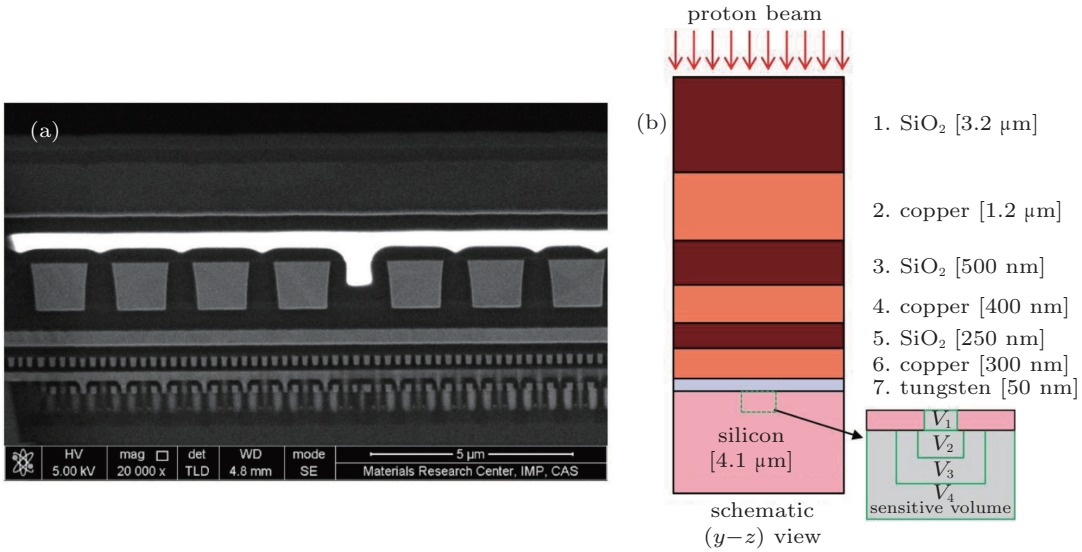


Fig. 1. (color online) (a) The SEM view of the passivation and metallization layers. (b) Schematic chart of the multilayer structure and weighted SV model used in CRÈME-MC simulation of the device, with a cubic surface area of 10 μm × 10 μm. Not drawn exactly in accordance with the scale.

The SEU occurs if and only if the deposited charge exceeds the Q_c, the $\mathrm{LET_{th}}$ represents the threshold LET to cause an SEU, and the $D_{\mathrm{SV}}(\mu\mathrm{m})$ is the depth of the SV. As shown in Fig. 1(b), a weighted SV model[14,15] was constructed and used to model the response of the 65-nm SRAM chip to proton irradiation. The weighted SV model contains four SVs ($\mathrm{SV_1}$, $\mathrm{SV_2}$, $\mathrm{SV_3}$, and $\mathrm{SV_4}$), the sizes of these SV models are 0.2 μm × 0.2 μm × 0.1 μm, 0.5 μm × 0.5 μm × 0.2 μm, 1 μm × 1 μm × 0.5 μm, and 2.2 μm × 2.2 μm × 1 μm, respectively. The charge collected at device node i is to sum the energy deposited in N_i sensitive volumes scaled by a weight $\alpha_{i,j}$ for $(0 \leq j < N_i)$ and the mean ionization potential $I(Z)$ of the material (3.6 eV/ehp in silicon). The value of α is obtained from Ref. [14] and the size of each SV is gained by fitting based on the experimental results. The following physical processes were included in the simulation: HadronElastic, Decay, EmStandardScreened, NucleonHadronic, HadronInelastic, particles, PiKInelastic, and IonInelasticLAQGSM. The chip was irradiated by proton beam from the surface of it as shown in Fig. 1(b). More than 10^7 particles are used to penetrate into the chip for each simulation. In order to verify the effectiveness of the model presents here, experiment results are also carried out to compare with the simulated results. Details of the experiment facilities and the energies used are given in Table 1.

Table 1. Test facilities and beam energies used in the experiments.

Facility	Initial proton energy/MeV	Proton energy at chip surface/MeV
EN-18	1∼8	0.3∼8
PSI-PIF	200	16∼200

At EN-18 tandem accelerator (Peking University), the primary beam energy is from 1 MeV to 8 MeV. Low energy proton beams (down to 0.3 MeV) were obtained by using an aluminum degrader in the beam path. The experiment of SEU induced by high proton energy (16 MeV–200 MeV) was conducted using the Proton Irradiation Facility in the Paul Scherrer Institute (PSI-PIF).

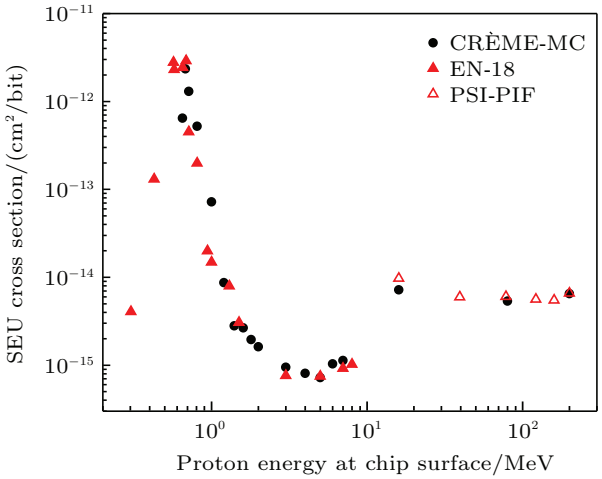


Fig. 2. (color online) The tested (red triangle symbols) and simulated (black circle symbols) SEU cross section as a function of proton energy at the chip surface for the 65-nm SRAM. Simulated SEU cross section are calculated directly by CRÈME-MC except for the proton energy is 16 MeV and 39 MeV. Error bars in this figure are smaller than the data symbols.

Figure 2 gives the tested and simulated SEU cross sections versus proton energy at the chip surface for the 65-nm SRAM. The CRÈME-MC tool cannot be used to calculate the SEU cross section for the initial proton energy of 200 MeV with the 43-mm Cu degrader (16 MeV at the chip surface) due to the existence of some defects in this tool, so all simulated SEU cross sections are calculated directly by CRÈME-MC except for the proton energy which is 16 MeV. The SEU cross section for the proton energy 16 MeV is calculated based on the energy spectrum (calculated by SRIM-2008) for the initial proton energy 200 MeV with the 43-mm Cu degrader. The

impact of degraders is also considered in the test and simulation, and it is clear that the simulated results are in good agreement with the experiment results. For instance, the SEU cross sections both reach the maximum value when the proton energy is up to 0.68 MeV (caused by direct ionization[1]), and drop rapidly with the increase of proton energy, finally the SEU cross sections increase again and reach saturation as the proton energy goes up to 200 MeV. The SEU cross sections resulting from low energy proton direct ionization are about three orders of magnitude than from high energy proton indirect ionization. It should to be emphasized that degraders are employed in both the testing and the simulation. The use of a degrader will cause energy straggling, and the detailed analysis of the impact of energy straggle on proton-induced SEU will be summarized below.

3. Physics of energy straggling

The incident protons in the device will no longer be at the same position, but will be spread over a certain volume. This is due to a large number of uncorrelated random collisions along the track, and the protons range and energy will have a Gaussian distribution[16,17]

$$f(x) = \frac{1}{\sqrt{2\pi}\sigma} \exp\left(-\frac{(x-\mu)^2}{2\sigma^2}\right), \tag{2}$$

where the parameter μ represents the mean value of the proton range or energy distribution, and σ is the root-mean-square (r.m.s.) deviation, given by

$$\sigma^2 = \langle (x-\bar{x})^2 \rangle = \int (x-\bar{x})^2 f(x)\,\mathrm{d}x. \tag{3}$$

The quantity $f(a)\,\mathrm{d}x$ represents the probability that x takes a value between a and $(a+\mathrm{d}x)$, so equation (2) has the following property

$$\int_{-\infty}^{+\infty} f(x)\,\mathrm{d}x = 1. \tag{4}$$

The width of such a distribution is often characterised by its full width at half maximum (FWHM). The FWHM of the distribution is used to quantify the absolute straggling

$$S_a = \mathrm{FWHM} = \sigma\sqrt{8\ln 2} = 2.355\sigma, \tag{5}$$

and the relative straggling is given by

$$S_\mathrm{r} = \pm\frac{\mathrm{FWHM}}{2\mu} \times 100\%. \tag{6}$$

4. Discussion

4.1. Energy straggling after different thicknesses of degraders

When protons penetrate into the device, the linear energy transfer (LET) and the deposited charge usually increase up to the end of the range and reach a maximum before the proton energy drops to zero. Figure 3 shows how the LET increases while the 1-MeV proton traverses in silicon. As shown in the figure, when protons with a certain energy enter the device, the following three cases exist: (i) the proton range in the device is not enough to reach the SV of the device; (ii) the Bragg peak of the proton is located in the SV of the device exactly; (iii) the proton range is greater than the position of the SV. By changing the incident proton energy, one can increase or decrease the range of the proton in the device. For a mono-energetic proton beam incidenting the SV, only one of the above three cases can happen. However, all three cases are likely to present at the same time in the actual situation because of energy straggle.

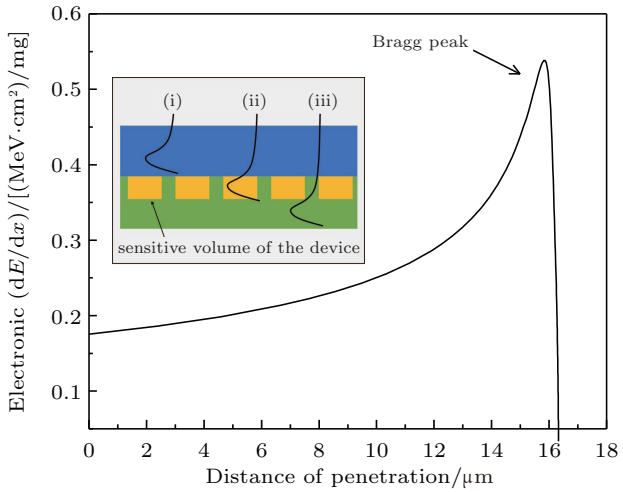


Fig. 3. (color online) Bragg curve of 1.0-MeV proton penetrating into silicon. The inset shows the three possible cases for proton incident to the chip: (i) the proton range is not enough to reach to the SV of the device; (ii) the Bragg peak of the proton is located in the SV of the device exactly; (iii) the proton range is larger than the position of the SV.

Number of protons as a function of proton energy after the different thickness of degraders and proton range in the device is shown in Fig. 4 and Fig. 5, respectively. The comparison of different initial proton beams reveals that the use of a degrader will have a great impact on the proton energy straggle and range straggle. The trend of energy straggling for different thicknesses of aluminum is further studied. The absolute straggling and the relative straggling of the proton range were calculated from Fig. 5 and plotted as a function of the thicknesses of the aluminum degrader in Fig. 6.

As depicted in Fig. 5, the proton range in the chip is very concentrated in the SV and the number of protons exhibit a sharp peak for the case of initial proton energy which is 0.68 MeV (without degrader), the absolute and relative range straggling is also very low. The peak of proton counts broadened and the value of range straggle increased (as shown in Fig. 6) as the initial proton energy becomes higher. The 0.68-MeV energy on the surface of the chip is right to make the proton reach the SV, so if the peak of counts spread,

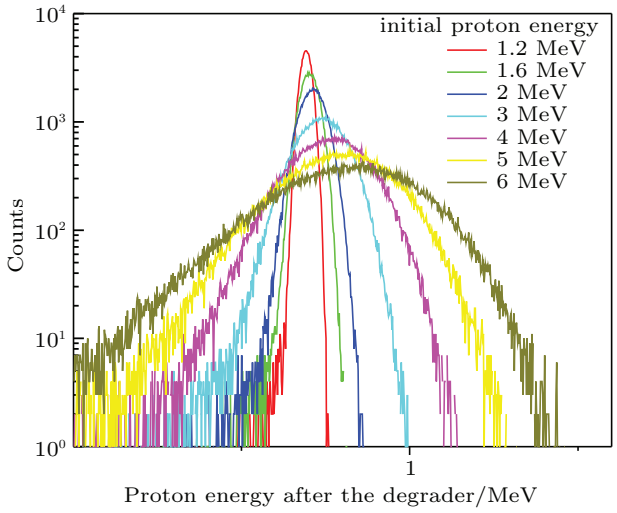


Fig. 4. (color online) Number of protons as a function of proton energy after different thicknesses of degraders. The mean value of proton energies after degraders are the same (0.68 MeV). The higher the initial proton energy, the thicker the added degrader.

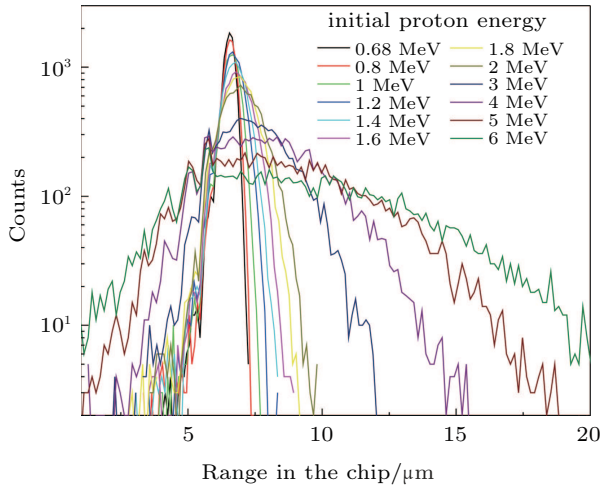


Fig. 5. (color online) The distribution of proton range in the chip (simulated by SRIM-2008). Each energy represents the initial proton energy, and through adding different thicknesses of aluminum degrader, the energies at the chip surface are the same (0.68 MeV).

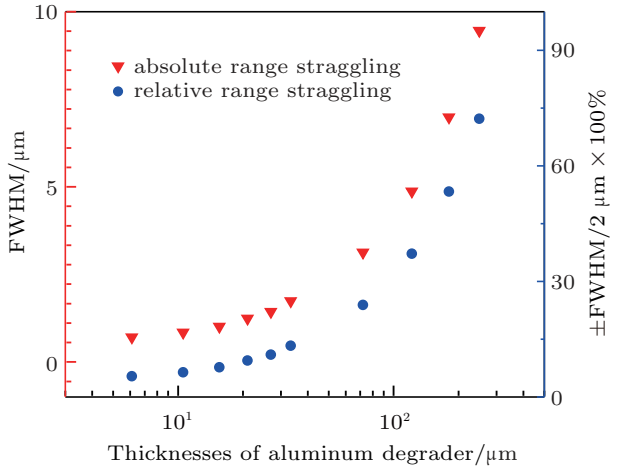


Fig. 6. (color online) Absolute range straggling (red down-triangle symbols) and relative range straggling (blue circle symbols) of proton range in the device as a function of the thickness of aluminum degrader. The proton energies at the chip surface are the same (0.68 MeV).

that means less protons could induce SEU for this device. Similarly, when we use degraders to make the proton energy on the device be 0.3 MeV, it is not a highly monoenergetic beam but a distribution. This phenomenon explained why the proton range seems not deep enough to reach the SV but we still detected SEU in this device (see Fig. 2).

4.2. Impact of energy straggle on the device response

As shown in Fig. 7, the number of protons as a function of the deposited charge in SV has been obtained by using CRÈME-MC. There are four peaks existing on each curve of the deposited charge which are caused by the weighted SV that contained four different SVs.

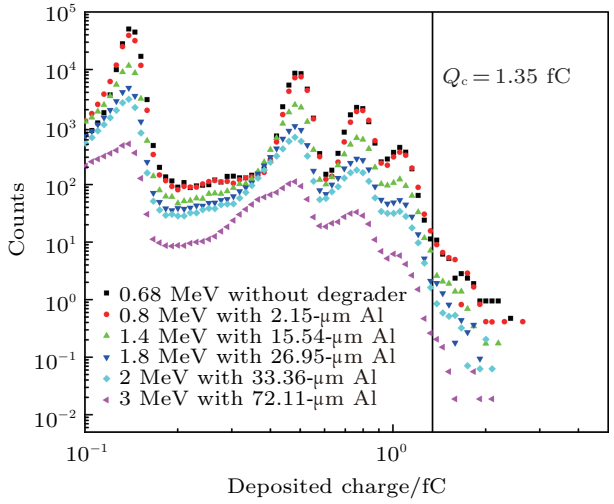


Fig. 7. (color online) The CRÈME-MC simulated number of protons as a function of the deposited charge in the SV of the device. Through adding a certain thickness of degrader, the proton energy at the chip surface is the same (0.68 MeV).

As depicted in Fig. 8, different SVs have a great impact on the deposited charges calculation. The curve in Fig. 7 demonstrates that the initial proton energy with a certain thickness of degrader has a significant impact on the counts of the deposited charge. In addition, the SEU cross section of the device (Fig. 9) induced by different initial protons with a certain thickness of Al degrader is also calculated. As can be seen from Fig. 9, the differences of SEU cross sections of different initial proton energies are obvious and it indicates that about one order of magnitude difference appears as the initial proton energy goes up from 0.68 MeV to 2 MeV. In our experiments, the initial proton energy of 1 MeV has been used (with a 6-μm aluminum degrader). The simulated SEU cross section for initial proton energy of 1 MeV is about 2.4×10^{-12} cm^2/bit, and this result is in good agreement with our experimental result (2.9×10^{-12} cm^2/bit).

As depicted in Fig. 2, a slight increase of the experimental SEU cross section appears when the proton energy is around 16 MeV (200-MeV initial proton energy with 43-mm Cu

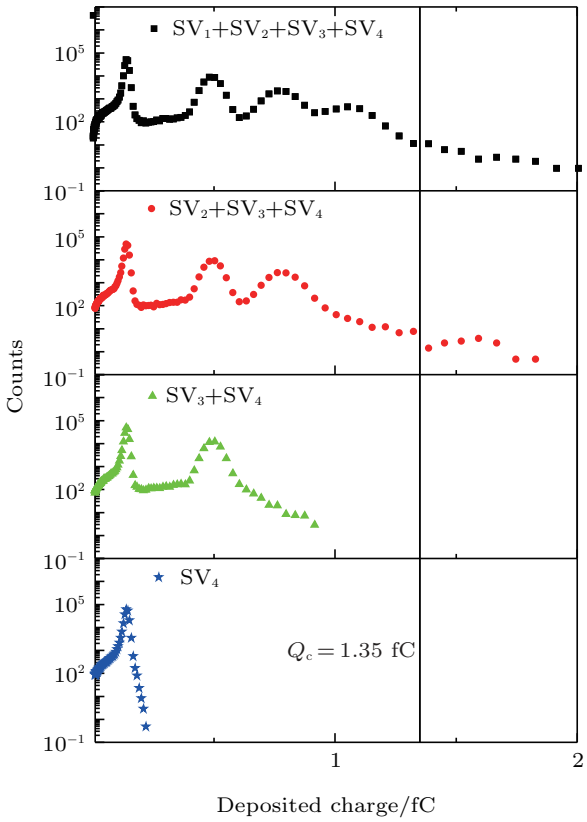


Fig. 8. (color online) The impact of weighted SVs on the deposited charge in the SV for the initial proton energy on the chip surface is 0.68 MeV.

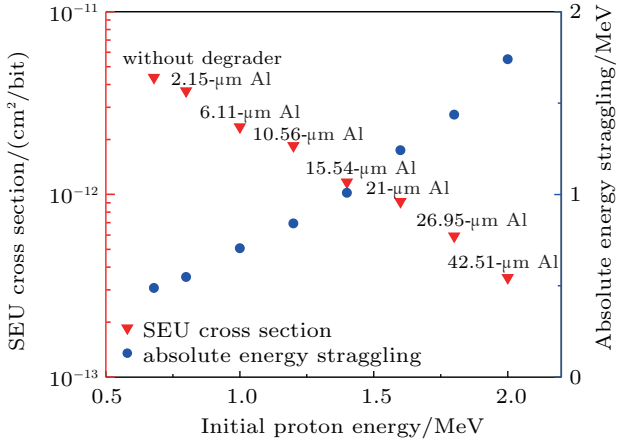


Fig. 9. (color online) The simulated SEU cross section (red down-triangle symbols) of the device and the absolute energy straggling (blue circle symbols) as a function of initial proton energy, the proton energy at the chip surface is the same (0.68 MeV).

degrader). To explore this abnormal phenomenon, the proton energy distributions and the absolute proton energy straggling (FWHM) are calculated, as illustrated in Fig. 10. The proton primary beam energy in the experiments is 200 MeV, and the other proton energies used in the test are obtained by adding different thicknesses of copper degraders. It is demonstrated that the energy distribution is widened and the absolute energy straggling increases with the increase of the thickness of the copper degraders. When the proton energy drops to 16 MeV by adjusting the copper degrader with thickness of 43 mm, the proton energy distribution shows that some of the protons energies are less than 1 MeV. This means that these protons can induce SEU in this device through direct ionization. Moreover, as figure 2 shows, the cross section of SEU induced by the low energy proton direct ionization can be three orders of magnitude than that of the high-energy proton. This explains why the SEU cross section is shown to slightly increase when the energy drops to 16 MeV through adding the copper degrader.

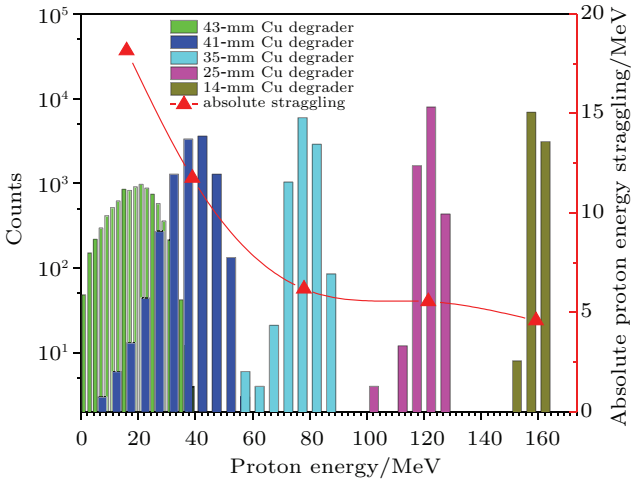


Fig. 10. (color online) The energy distribution on the device surface and the absolute energy straggling (red up-triangle symbols) of the proton energy with different thicknesses of copper. Initial proton energies are the same (200 MeV).

5. Conclusion

In this work, the impact of energy straggle on proton-induced SEU in nanodevices has been investigated by using SRIM and CRÈME-MC. Under the condition of the same proton energy on the chip surface but with different initial proton energies and degraders, the simulated results show that the influence of energy straggle on proton-induced SEU test needs to be further considered. Simulated results showed that the proton range and energy straggle increases with degrader thickness increase. Detailed studies with low energy proton and high energy proton indicate that when conducting an SEU test on a nanodevice, the impact of energy straggle is mainly reflected in the following three aspects. First, the energy straggle will result in erroneous threshold energy of proton-induced SEU. Second, the energy straggle will significantly lower the peak value of the proton-induced SEU cross section through direct ionization. Third, it may change the SEU cross section curve trend for high energy proton.

Acknowledgment

The authors are thankful to the accelerator staff of the Institute of Heavy Ion Physics of the Peking University and PSI-PIF for providing the irradiation facilities.

References

[1] Heidel D F, Marshall P W, LaBel K A, Schwank J R, Rodbell K P, Hakey M C, Berg M D, Dodd P E, Friendlich M R, Phan A D, Seidleck C M, Shaneyfelt M R and Xapsos M A 2008 *IEEE Trans. Nucl. Sci.* **55** 3394

[2] Loveless T D, Jagannathan S, Reece T, Chetia J, Bhuva B L, McCurdy M W, Massengill L W, Wen S J, Wong R and Rennie D 2011 *IEEE Trans. Nucl. Sci.* **58** 1008

[3] Heidel D F, Marshall P W, Pellish J A, Rodbell K P, LaBel K A, Schwank J R, Rauch S E, Hakey M C, Berg M D, Castaneda C M, Dodd P E, Friendlich M R, Phan A D, Seidleck C M, Shaneyfelt M R and Xapsos M A 2009 *IEEE Trans. Nucl. Sci.* **56** 3499

[4] Cannon E H, Cabanas-Holmen M, Wert J, Amort T, Brees R, Koehn J, Meaker B and Normand E 2010 *IEEE Trans. Nucl. Sci.* **57** 3493

[5] Seifert N, Gill B, Pellish J A, Marshall P W and LaBel K A 2011 *IEEE Trans. Nucl. Sci.* **58** 2711

[6] Schwank J R, Shaneyfelt M R and Dodd P E 2013 *IEEE Trans. Nucl. Sci.* **60** 2101

[7] Dodds N A, Schwank J R, Shaneyfelt M R, Dodd P E, Doyle B L, Trinczek M, Blackmore E W, Rodbell K P, Gordon M S, Reed R A, Pellish J A, LaBel K A, Marshall P W, Swanson S E, Vizkelethy G, Deusen S V, Sexton F W and Martinez M J 2014 *IEEE Trans. Nucl. Sci.* **61** 2904

[8] Pellish J A, Marshall P W, Rodbell K P, Gordon M S, LaBel K A, Schwank J R, Dodds N A, Castaneda C M, Berg M D, Kim H S, Phan A M and Seidleck C M 2014 *IEEE Trans. Nucl. Sci.* **61** 2896

[9] Luo Y H, Zhang F Q, Wang Y P, Wang Y M, Guo X Q and Guo H X 2014 *Acta Phys. Sin.* **65** 068501 (in Chinese)

[10] Luo Y H, Zhang F Q, Guo H X, Guo X Q, Zhao W, Ding L L and Wang Y M 2015 *Acta Phys. Sin.* **64** 216103 (in Chinese)

[11] Ziegler J F, Ziegler M D and Biersack J P 2014 2010 *Nucl. Instrum. Methods Phys. Res. Sect. B* **268** 1818

[12] Sierawski B D, Mendenhall M H, Weller R A, Reed R A, Adams J H, Watts J W and Barghouty A F 2010 *IEEE Nuclear Science Symposium & Medical Imaging Conference*, October 30–November 6, 2010, Knoxville, USA, p. 1258

[13] http://www.cypress.com/?docID≒46467

[14] Warren K M, Sierawski B D, Weller R A, Reed R A, Mendenhall M H, Pellish J A, Schrimpf R D, Massengill L W, Porter M E and Wilkinson J D 2007 *IEEE Electron Dev. Lett.* **28** 180

[15] Sierawski B D, Pellish J A, Reed R A, Schrimpf R D, Warren K M, Weller R A, Mendenhall M H, Black J D, Tipton A D, Xapsos M A, Baumann R C, Deng X, Campola M J, Friendlich M R, Kim H S, Phan A M and Seidleck C M 2009 *IEEE Trans. Nucl. Sci.* **56** 3085

[16] Tavernier P S 2010 *Experimental Techniques in Nuclear and Particle Physics* (Berlin: Springer) pp. 167–208

[17] Zhang Z G, Liu J, Hou M D, Sun Y M, Zhao F Z, Liu G, Han Z S, Geng C, Liu J D, Xi K, Duan J L, Yao H J, Mo D, Luo J, Gu S and Liu T Q 2013 *Chin. Phys. B* **22** 096103